Stability of the high-spin ground state in alternant π-conjugated organic molecules

Bhabadyuti Sinha, I. D. L. Albert, and S. Ramasesha
Solid State and Structural Chemistry Unit, Indian Institute of Science, Bangalore 560 012, Karnataka, India
(Received 14 May 1990)

Alternant quantum cell models with unequal numbers of atoms on the two sublattices have been predicted to have a high-spin ground state. In this paper, we examine the stability of this high-spin ground state with respect to breaking the alternancy symmetry and distortion of the backbone conjugation. We find that in the Pariser-Parr-Pople (PPP) models and the Hubbard models with weak correlations, the ground state continues to be the high-spin state, even when alternancy symmetry is broken by introducing large site-energy differences. In the Hubbard model, for strong correlation strengths, the ground state switches from a high-spin to a low-spin state when large site-energy differences are introduced. The bond-order calculations in all these models shows that the low-spin state is susceptible to dimerization of the backbone. In the distorted chains, the low-spin state stabilizes to a greater extent leading to low-spin ground states at least in "soft" lattices. However, experience with one-dimensional systems suggests that the lattice distortion could occur unconditionally leading to low-spin ground state in infinitely long polymers. Thus, realization of organic ferromagnetics via high-spin polymers could be elusive.

I. INTRODUCTION

All known ferromagnetic materials, both natural and man-made, are primarily inorganic systems. The synthesis of an organic or molecular ferromagnet has been a challenge that has attracted considerable attention.[1] Although the early theoretical model for ferromagnetism in organic solids was based on the stacking of organic radicals so that in neighboring radicals the atoms with positive and negative spin densities are juxtaposed, thereby leading to incomplete spin cancellation,[2,3] it has been realized that such a model cannot lead to bulk ferromagnetism.[1] Currently there are two main avenues explored by experimentalists for obtaining an organic ferromagnet. The first has its origin in the model proposed by McConnell[4] for the formation of a dimer in the triplet ground state. In this model, the triplet state is stabilized relative to the singlet state by a configuration interaction with a triplet charge-transfer excited state; this excited state is lower in energy when compared to the singlet exited state due to the presence of degenerate partially occupied molecular orbitals. In low-dimensional organic charge-transfer systems, many variants of this model have been pursued, based on different stacking of the donor and acceptor units.[5–8]

The second approach, first suggested by Mataga,[9] is the synthesis of organic polymers in the high-spin ground state. Later, Ovchinnikov[10] showed that in alternant hydrocarbons (wherein the carbon atoms can be partitioned into two sublattices usually called the starred and the unstarred) if the number of atoms on the starred and unstarred sublattices are not equal, the ground state is a high-spin state with its spin given by half the absolute difference between the number of starred and unstarred atoms. Some small chain-length polymers in this category have indeed been synthesized and they are known to have a high-spin ground state.[11]

In this paper we present the results of a detailed study of the energy-level spectrum of a class of polymers that are expected to possess a high-spin ground state. Our study is primarily concerned with the stability of the high-spin ground state in the limit of long chain lengths and with respect to the breaking of the alternancy symmetry. Since conjugated systems are known to be strongly correlated, we have modeled them employing a Pariser-Parr-Pople (PPP) model Hamiltonian.[12,13] However, to understand the effect of correlations on the excitation spectrum, we have also studied Hubbard models[14] with varying on-site repulsion energy U.

In order to have reliable extrapolations of the excitation gaps in the spectrum to the limit of infinite chain length, it is essential that model exact calculations be carried out on as large a system size as possible. In the PPP and the Hubbard models, every given orbital or site has four possible states and hence the dimension of the complete Hilbert space spanned by a model Hamiltonian with N sites goes up rapidly with N ($\cong 4^N$). Therefore, a model exact computation in these models is typically restricted to about 12 carbon atoms. However, it is well known that both these model Hamiltonians, in the half-filled case and at large correlation energies, can be represented by the spin-half antiferromagnetic Heisenberg Hamiltonian.[15] The Heisenberg Hamiltonian eliminates charge degrees of freedom by fixing the orbital occupancy of each orbital to one. Therefore at each site there are only two possibilities, namely, the spin can be either up or down. This restriction results in a slower increase in the dimensionality of the complete Hilbert space of the Hamiltonian with an increase in the system size N ($\cong 2^N$). Therefore, in the large correlation limit we can obtain a model exact solution of systems with up to 22 sites. This leads to greater reliability in the extrapolation of the excitation gaps in the system.

II. MODEL HAMILTONIANS AND COMPUTATIONAL DETAILS

The polymer on which we have carried out the calculations is shown in Fig. 1. The PPP model Hamiltonian that we have employed for modeling this polymer is given by

$$H_{\mathrm{PPP}}=t_0\sum_{\langle ij\rangle}\sum_{\sigma}(a_{i\sigma}^{*}a_{j\sigma}+\mathrm{H.c.})+\sum_i \varepsilon_i n_i + U\sum_i \hat{n}_i(\hat{n}_i-1)/2+\sum_{i>j}V_{ij}n_i n_j \ , \tag{1}$$

where ε_i is the site (orbital) energy of site (orbital) i and t_0 is the transfer integral set to 2.4 eV in all cases except where specified. $a_{i\sigma}^{*}$ ($a_{i\sigma}$) creates (annihilates) an electron in the spin orbital i with spin σ. The geometry of the polymer, necessary for calculating the intersite interaction energy is as shown in the figure. In the PPP model, the on-site repulsion energy U is set to 11.26 eV and the orbital energies ε_i on the carbon atoms (atoms No. 2, 5, 8, etc., in Fig. 1) and the dangling carbon atoms (atoms No. 3, 6, 9, etc. in Fig. 1) are varied between 0 and 2 eV to mimic substitutions as well as to take into account the different stabilities of the carbon atoms with different numbers of C—C bonds. The intersite potential energy is parametrized using Ohno parametrization,[16]

$$V_{ij}=U(1+0.6117r_{ij}^{2})^{-1/2} \ . \tag{2}$$

In the Hubbard model the intersite interaction term is identically zero and we vary the parameters U/t_0 and ε_i/t_0 in our studies.

The Heisenberg Hamiltonian employed in these studies is given by

$$H_{\mathrm{spin}}=J\sum_{\langle ij\rangle}(\mathbf{s}_i\cdot\mathbf{s}_j-\tfrac{1}{4}) \ , \tag{3}$$

where J is the exchange integral and the summation is over all the nearest-neighbor spin bonds.

All the Hamiltonians in Eqs. (1) to (3) have the property that they conserve total spin. Therefore, we have employed a valence-bond (VB) basis for carrying out all our computations. The VB basis has the obvious advantage that the states are spin labeled and also leads to smaller dimensions of the exact Hamiltonian matrices that represent these Hamiltonians. A complete and linearly independent VB basis can be generated by employing the modified Rumer-Pauling rules.[17] However, the nonorthogonality of the basis leads to matrices that are nonsymmetric, though real. The low-lying eigenvalues and eigenfunctions are obtained using a numerical scheme due to Davidson[18] and Rettrup.[19]

The polymeric systems that we are dealing with are not topologically one-dimensional and contain transfer or exchange terms between nonconsecutively labeled atoms. Such exchanges or electron transfers, termed long bonds, can lead to VB diagrams that violate the Rumer-Pauling rules. Although the generation of such "illegal" VB diagrams can be avoided by employing the computation relations

$$(i,j)=[(i,k),(k,j)]_{-} \ , \tag{4a}$$

$$\mathbf{s}_i\cdot\mathbf{s}_{i+2}=2[\mathbf{s}_i\cdot\mathbf{s}_{i+1},\mathbf{s}_{i+1}\cdot\mathbf{s}_{i+2}]_{+} \ , \tag{4b}$$

where $(i,j)=(a_{i\alpha}^{*}a_{j\alpha}+a_{i\beta}^{*}a_{j\beta})$ and $\mathbf{k}$ is the intervening orbital. We find this procedure in general to be slow and cumbersome due to the presence of a large number of long bonds in our system. Instead, we use the following relation between "legal" and "illegal" diagrams repeatedly:

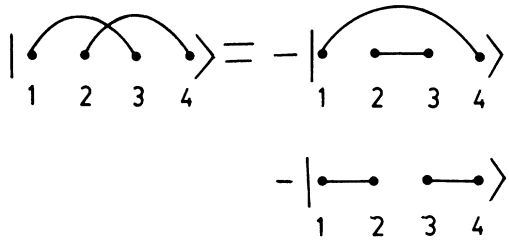

(5)

where a line between sites i and j ($i<j$) represents a singlet pairing of the spins on the sites i and j, namely $[(a_{i\alpha}^{*}a_{j\beta}^{*}-a_{i\beta}^{*}a_{j\alpha}^{*})/\sqrt{2}]|0\rangle$. In the case of high-spin states ($S>0$), where we employ phantom sites,[20] this procedure is particularly useful since the presence of phantom sites leads to long bond connections with at least $2S$ intervening sites in cyclic systems.

The properties of the states that we have calculated include bond orders and spin densities in the PPP, Hubbard, and Heisenberg models. In the PPP and Hubbard models, two functions in the VB basis are orthogonal when the occupancy of the sites in the two functions are not identical. This property can be used to advantage to block diagonalize the VB basis in the course of calculating spin densities and bond orders. However, in the spin models, for a given total spin, any two VB functions are strictly nonorthogonal. In such a situation, calculation of the spin bond orders and spin densities becomes computationally prohibitive for large systems. We have, therefore, transformed the eigenfunctions in the VB basis to the Slater determinantal basis for calculating spin densities. The spin densities in the Hückel model which can be calculated analytically provide a convenient numerical check on our method for the PPP and Hubbard models. The procedure for spin densities of the Heisenberg model are verified by calculating the spin density of the Hubbard chain at very large U/t and comparing the results with the spin density of the corresponding Heisenberg chain. The bond orders for the various bonds are calculated using numerical differentiation. In this procedure, for each bond the total energy is calculated twice, once with the exchange integral for the bond in question being set to $J+\delta$ and the second time the same being set to $J-\delta$, while all other exchange integrals remain the same. The bond order of the band is now given by $[E(J+\delta)-E(J-\delta)]/2\delta$ and this definition yields twice the value obtained from the usual definitions.

In Tables I(a) and I(b) we present the dimensionalities of the various subspaces we have encountered in our calculations. The largest matrix that we have dealt with is for the case of $S=3$ in the 22-spin polymer. The complete and linearly independent Hilbert space spanned in this case has a dimension of 149 226 and the Hamiltonian matrix has almost 2.2 million nonzero elements. The

TABLE I. (a) Dimensions $P(S)$ of the complete Hilbert spaces spanned by the PPP and Hubbard Hamiltonians for different system sizes N and total spin S. (b) Dimension $P(S)$ of the complete Hilbert space spanned by the Heisenberg spin-$\frac{1}{2}$ Hamiltonian for different system sizes N and total spin S.

N	S	$P(S)$	S	$P(S)$	S	$P(S)$	S	$P(S)$
				(a)				
6	0	175	1	189	2	35		
7	$\frac{1}{2}$	784	$\frac{3}{2}$	392	$\frac{5}{2}$	48		
9	$\frac{1}{2}$	8 820	$\frac{3}{2}$	5 760	$\frac{5}{2}$	1 215		
10	0	19 404	1	29 700	2	12 375	3	1 925
				(b)				
7	$\frac{1}{2}$	14	$\frac{3}{2}$	14	$\frac{5}{2}$	6		
10	0	42	1	90	2	75	3	35
13	$\frac{1}{2}$	429	$\frac{3}{2}$	572	$\frac{5}{2}$	429	$\frac{7}{2}$	208
16	0	1 430	2	3 640	3	2 548	4	1 260
19	$\frac{1}{2}$	16 796	$\frac{5}{2}$	23 256	$\frac{7}{2}$	15 504	$\frac{9}{2}$	7 752
22	0	58 786	3	149 226	4	95 931	5	48 279

lowest two eigenvalues for this case take about 18 h of CPU time on a micro VAX II system on which all these calculations were carried out.

III. RESULTS AND DISCUSSION

The energy of the expected ground state with spin S_g, where $S_g=|n_s-n_0|/2$ (n_s being the number of starred atoms and n_0 being the number of unstarred atoms), has been calculated for each system size. To study the stability of this high-spin state, we have also calculated the energies of the $S=0$ states in polymers with an even number of sites and the energies of the $S=\frac{1}{2}$ states in polymers with an odd number of sites. Other excitation gaps studied include the excitation energies to states with spin $S=S_g\pm1$. The system sizes that we have studied range from six to ten sites in the case of the PPP and Hubbard models and from seven to 22 spins in the spin models. In the PPP model we have studied the stability of the high-spin state with respect to the breaking of the electron-hole symmetry. The symmetry breaking is achieved by introducing different site energies for different sites. In the Hubbard model we have also studied the stability of the high-spin state as a function of the strength of on-site electron correlations. We have calculated the bond orders of different spin states in all the models. Based on the bond-order pattern, we have carried out calculations of the distorted systems to study the effect of distortions on the excitation gaps and the stability of the high-spin state in the system. We discuss in detail the results pertaining to these studies in Secs. III A–III C.

TABLE II. Excitation gaps in the PPP model and Hubbard model with $U/t=4.0$ for different N and site energies $|\varepsilon|=0.0$.

Model	System size	S_G	$E(S_G)$	$E(S=0,\frac{1}{2})$	$E(S_G+1)$	$E(S_G-1)$
PPP	6	1	0.0000	0.7673	3.6158	Same as
			2.1924	1.0984	5.7716	in $S=0$
	7	$\frac{3}{2}$	0.0000	0.2937	5.1998	Same as
			3.3344	1.0300	6.0330	in $S=\frac{1}{2}$
	9	$\frac{3}{2}$	0.0000	0.4550	4.7563	Same as
			2.9408	0.6280	5.4025	in $S=\frac{1}{2}$
	10	2	0.0000	0.3633	4.7797	0.1660
			3.0215	1.1753	5.5726	0.5373
Hubbard	6	1	0.0000	0.4349	0.9948	Same as
			0.6906	0.5125	1.6732	in $S=0$
	7	$\frac{3}{2}$	0.0000	0.1184	1.4117	Same as
			1.0411	0.4033	1.6774	in $S=\frac{1}{2}$
	9	$\frac{3}{2}$	0.0000	0.2125	1.2866	Same as
			0.9782	0.5171	1.6114	in $S=\frac{1}{2}$
	10	2	0.0000	0.1548	1.2981	0.0692
			0.9501	0.4250	1.5385	0.2075

A. Magnetic excitations in alternant models

In Table II we present the excitation gaps in the PPP and Hubbard models. In these models all the site energies ε_i are set to zero. All the transfer integrals in the PPP model are set to the molecular value of 2.4 eV appropriate to the C—C π bond in benzene. In the Hubbard model, the ratio U/t is varied, with the transfer integral t fixed at 1.0 eV for all the bonds. While the seven- and ten-site models are solved using open boundaries, the six- and nine-site models are solved using a cyclic boundary, resulting in the inclusion of a 1–5 transfer term in the six-site case and a 1–8 transfer term in the nine-site Hamiltonians. The geometries of the polymers, which determine the interaction energies in the PPP model, are always taken to correspond to the free-boundary case as shown in Fig. 1.

From Table II we notice that in all the cases the state with spin S_g is the ground state. The lowest-energy excitation is to the state with spin S_g-1. The excitation energy to the singlet (if the number of sites is even) or the doublet state (if the number of sites is odd) is comparable to the excitation energy to the state with spin S_g-1 and is substantially lower than that for the excitation to the state with spin S_g+1. The excitation energy to the first excited state with spin S_g is also much larger than the energy needed to excite the system to the $S=0$ or $\frac{1}{2}$ state. The excitation energies show a systematic decrease with an increase in the system size. Within the PPP and the Hubbard models, it is not possible to obtain a reliable extrapolation of the excitation gap to the infinite limit because of the limited size of the system for which exact calculations can be carried out. However, in the spin models, we can carry out exact calculations on much larger systems. Both the PPP and the Hubbard models in the limit of strong correlations map onto the Heisenberg model.

To obtain reasonable extrapolations of the magnetic gap, we have carried out calculations on Heisenberg systems with up to 22 spins. In all cases, we have employed open boundary conditions. In Fig. 2 is shown the variation of the magnetic gap and excitation gap to the lowest state with spin S_g-1 as a function of the inverse system size. We have two different dependences corresponding to half-integer and integer spin values. In the infinite system size limit, the gaps in both cases should converge to the same value. This restriction provides an estimate of the error in the extrapolations. The magnetic gap in units of J is 0.061 ± 0.007. Thus, the high-spin state remains the ground state even in the infinite size limit. The excitation energy to the S_g-1 state decreases rapidly. The dependence not being linear, we cannot estimate this gap in the infinite limit. But it appears that the two states become degenerate to $O(N^{-1})$ in the infinite polymer. The excitation gap to the state with spin S_g+1, on the other hand, remains finite and large in the infinite limit (Fig. 3).

In the case of the Hubbard model, we have also studied the dependence of the magnetic gap on U/t, the ratio of correlation strength to the transfer integral. In the limit of $U/t=0$, all the lowest-energy states in the subspaces with spin $S<S_g$ are degenerate since the highest occupied molecular orbitals are $2S_g$-fold degenerate. In the limit of $U/t\rightarrow\infty$ all the spin states are degenerate, the system being in the atomic limit. This degeneracy is lifted for finite U/t and from our calculations we find that the gap goes through a maximum (Fig. 4) when the bandwidth equals the correlation strength for all system sizes.

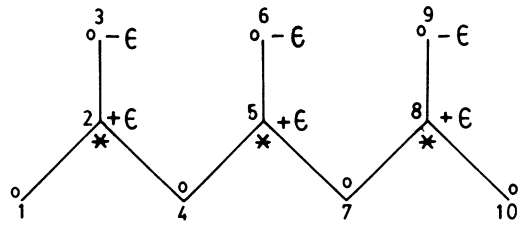

FIG. 1. Geometry of a typical polymer that has a high-spin ground state in an alternant model. ε are site energies. Starred (*) and unstarred (○) atoms belong to different sublattices. In calculations involving cyclic boundary conditions, site 10 is eliminated and a 1-8 bond is introduced without altering the site positions. All the bond angles are assumed to be 120° and all bond lengths in the undistorted system are set to 1.397 A.

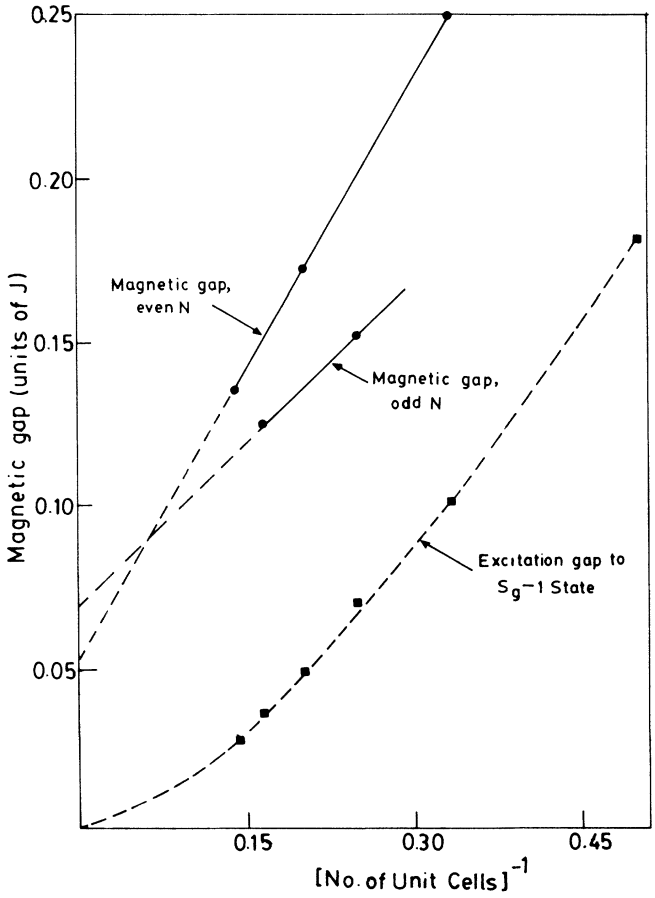

FIG. 2. Variation of the magnetic gap and excitation gap to the lowest state with spin S_g-1 as a function of the inverse system size in the Heisenberg model.

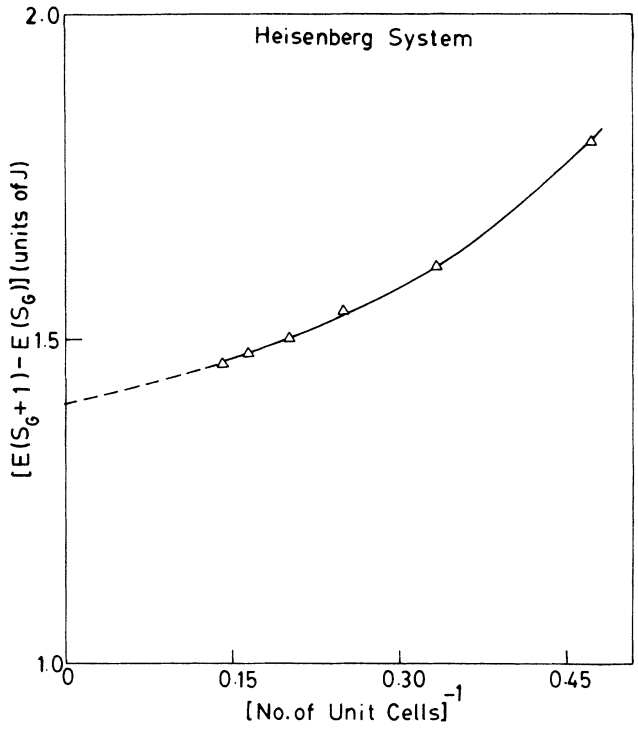

FIG. 3. The excitation gap to the lowest S_g+1 state as a function of the inverse system size in the Heisenberg model.

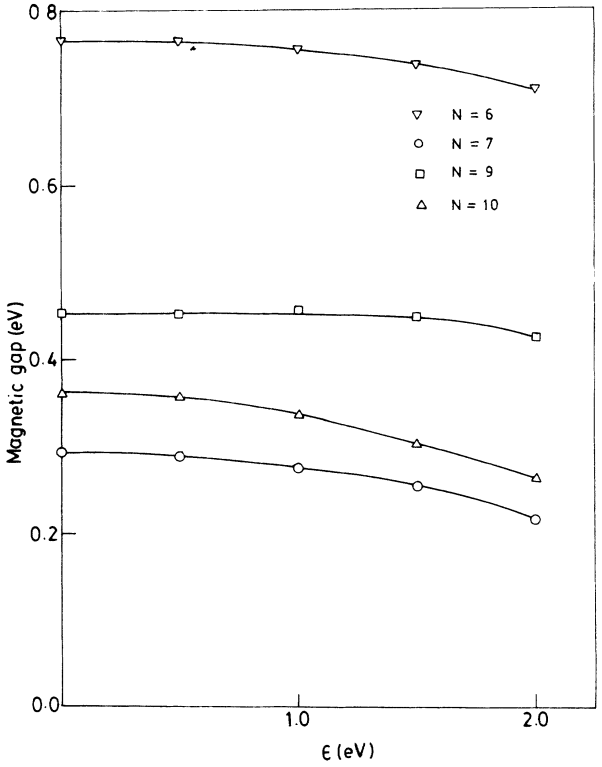

FIG. 5. Variation of the magnetic gap as a function of site energy $|\varepsilon|$ in the PPP model.

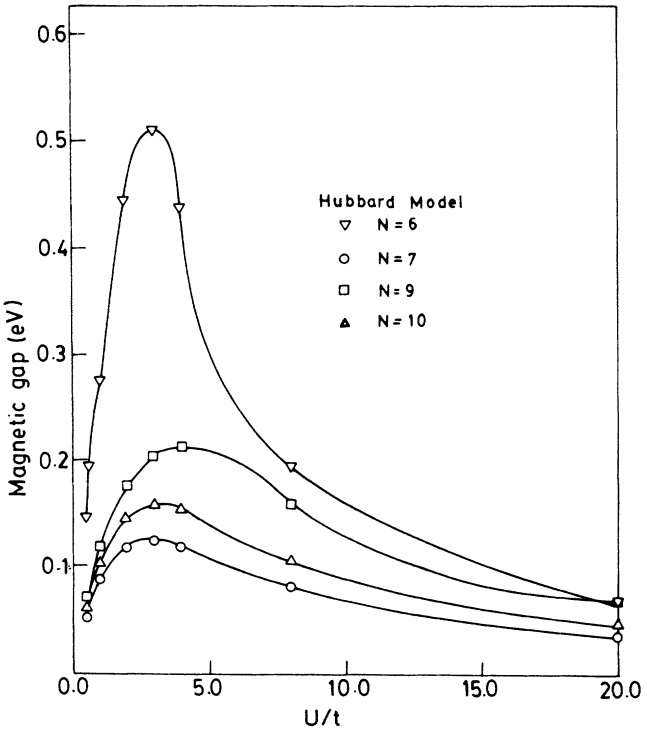

FIG. 4. Dependence of the magnetic gap on U/t, the ratio of the correlation strength to the transfer integral in the Hubbard model.

B. Magnetic excitations in nonalternant models

We break the alternancy symmetry in the Hubbard and PPP models by introducing nonequivalent site energies. The nodal sites that are connected to three atoms have a positive site energy while the dangling sites connected to a single atom have a negative site energy with reference to the carbon atoms connected to two atoms. We have assumed that the absolute value of the site energies, where they are nonzero, are the same. In the uncorrelated model, the introduction of the site energies leads to

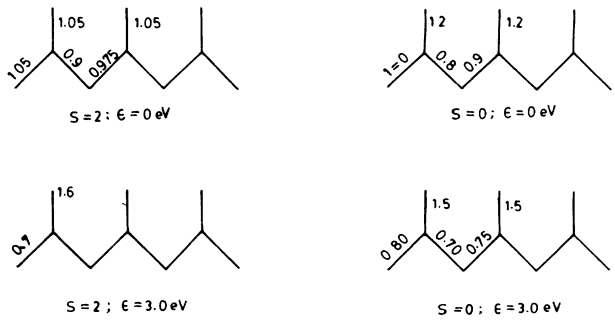

FIG. 6. Transfer integrals in the distorted polymer of ten sites for the $S=2$ and $S=0$ states with $|\varepsilon|=0$ and 3.0 eV in the Hubbard model.

TABLE III. Magnetic gap as a function of ε/t in the Hubbard model at $U/t=4.0$ for a system of seven sites with open boundary condition (A) and a system of six sites with cyclic boundary condition (B).

	Magnetic gap			Magnetic gap	
ε	A	B	ε	A	B
0.0	0.1184	0.4349	3.0	−0.0557	−0.1350
0.5	0.1170	0.4959	3.5	−0.0781	−0.1903
1.0	0.1087	0.4428	4.0	−0.0268	−1.7708
1.5	0.0831	0.3428	4.5	−0.0725	−0.1832
2.0	0.0400	0.1855	5.0	−0.0215	−0.1640
2.5	0.0013	0.0003	5.5	−0.0187	−0.1445

TABLE IV. (a) Bond orders in the PPP model for a system of ten sites with an open boundary condition (see Fig. 1 for site numbering). (b) Bond orders in the Hubbard model for a system of ten sites with an open boundary condition (see Fig. 1 for site numbering).

(a)

	$S_G=2$		$S=0$	
Bond	$\varepsilon=0.0$ eV	$\varepsilon=2.0$ eV	$\varepsilon=0.0$ eV	$\varepsilon=2.0$ eV
1-2	1.139	1.007	1.114	0.994
2-3	1.157	1.215	1.138	1.191
2-4	0.933	0.910	0.966	0.943
4-5	0.978	0.919	0.823	0.797
5-6	1.231	1.247	1.452	1.398

(b)

	$S_G=2$		$S=0$	
	$\varepsilon=0.0$ eV	$\varepsilon=3.0$ eV	$\varepsilon=0.0$ eV	$\varepsilon=3.0$ eV
1-2	0.941	0.494	0.914	0.556
2-3	0.941	1.158	0.914	1.101
2-4	0.808	0.495	0.837	0.548
4-5	0.843	0.499	0.669	0.512
5-6	0.984	1.158	1.189	1.142

TABLE V. Spin density in different spin states in the Hubbard ($U/t=4.0$) and PPP models of ten sites (Fig. 1 gives site numbering).

	PPP model			Hubbard model		
Site	$S=1$	$S=2$	$S=3$	$S=1$	$S=2$	$S=3$
1	0.1918	0.7004	0.8211	0.2147	0.7481	0.8533
2	−0.0898	−0.1920	0.0901	−0.1616	−0.3297	0.0183
3	0.1996	0.6894	0.8195	0.2147	0.7481	0.8533
4	0.4989	0.5779	0.5130	0.5571	0.6430	0.5406
5	−0.1635	−0.1925	0.5762	−0.2884	−0.3345	0.5265
6	0.5627	0.6409	0.9365	0.6385	0.7154	0.9433

TABLE VI. Magnetic gap in the distorted Hubbard ($U/t=4.0$) and PPP chains of ten sites. $|\varepsilon|$ is the site energy on the nodal and dangling sites.

		Magnetic gap	
	ε	Distorted	Undistorted
Hubbard	0.0	−0.0729	0.1548
model	3.0	0.3049	−0.0854
PPP	0.0	−0.4338	0.3633
model	2.0	−0.5016	0.2655

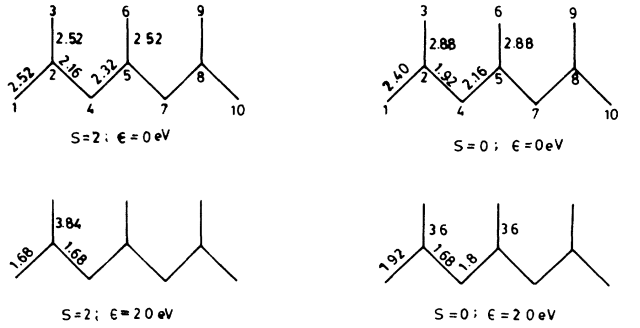

FIG. 7. Transfer integrals in the distorted PPP polymer of ten sites for $S=2$ and $S=0$ states with $|\varepsilon|=0$ and 2.0 eV.

the lifting of the degeneracy of the highest occupied molecular orbitals. Consequently, the low-spin state turns out to be the ground state with the excitation gaps to the high-spin states increasing for higher spin states. But in the PPP model we find (Fig. 5) that breaking electron-hole symmetry does not significantly alter the stability of the high-spin ground state. The magnetic gap shows a slight decrease with an increase in $|\varepsilon|$ and so does the excitation gap $[E(S_g)-E(s_g-1)]$, but the excitation to the state with spin S_g+1 increases with an increase in $|\varepsilon|$. Thus in real polymers, introducing electron pull and push groups will not have a significant effect on the ordering of the spin states. Indeed, a similar observation was made in the case of singlet excitation in push-pull polyenes.[21] In the Hubbard models, where we find that for $U/t=4.0$, the ground state switches from the high-spin state to the low-spin state for $\varepsilon/t>2.5$ (Table III). Although there is a slight anomaly in the stability of the low-spin state at $\varepsilon/t=4.0$, the ground state continues to be the low-spin state for all values of $\epsilon/t>2.5$ when the correlation strength is equal to the bandwidth.

C. Magnetic excitations in distorted polymers

The results discussed above pertain to polymers in which all the bonds are taken to be equivalent. However, it is known that one-dimensional systems are particularly unstable to distortions of the chain.[22] The distortion pattern can be known if we calculate the bond orders of all the bonds. In Tables IV(a) and IV(b), we present results of the bond-order calculations in the PPP model and the Hubbard model for different spin states in a polymer of ten sites. We find that for all the states, the bond order of the bonds between the nodal atom and the dangling atom are the largest. In the spin state S_g the bonds in the chain have weak alternation in the bond order while in the lowest-spin state this alternation along the chain is stronger. When large site-energy differences, $|\varepsilon|$, are introduced, the bonds along the chain have nearly uniform bond order in both the $S=0$ state and the $S=S_g$ state in the Hubbard model while the alternation does not show any significant changes in the PPP model.

The spin-density calculations (Table V) in the spin state S_g show that the spin on the nodal carbon atom is negative while that on the others is positive. The spin density is largest positive on the dangling carbon atoms. In the interior of the polymer, we find that the sum total of the spin densities of the dangling, nodal, and doubly bonded carbon atoms in a unit cell corresponds to one unpaired

TABLE VII. Bond order (A) of bonds (B) in the central unit cell in various spin states for different system sizes (Fig. 8 gives site numbering).

	$N=19$		$N=16$		$N=13$		$N=10$	
	B	A	B	A	B	A	B	A
$S=0,\frac{1}{2}$	11-12	0.752	8-9	0.807	8-9	0.760	5-6	0.869
	10-11	0.583	5-7	0.611	7-8	0.567	2-4	0.616
	11-13	0.602	7-8	0.524	8-10	0.563	4-5	0.455
$S=S_g-1$	11-12	0.733	8-9	0.739	8-9	0.742	5-6	0.754
	10-11	0.603	5-7	0.603	7-8	0.592	2-4	0.602
	11-13	0.598	7-8	0.597	8-10	0.596	4-5	0.568
$S=S_g$	11-12	0.787	8-9	0.729	8-9	0.725	5-6	0.723
	10-11	0.610	5-7	0.609	7-8	0.612	2-4	0.591
	11-13	0.610	7-8	0.610	8-10	0.615	4-5	0.615
$S=S_g+1$	11-12	0.433	8-9	0.348	8-9	0.339	5-6	0.221
	10-11	0.580	5-7	0.633	7-8	0.569	2-4	0.683
	11-13	0.515	7-8	0.513	8-10	0.421	4-5	0.404

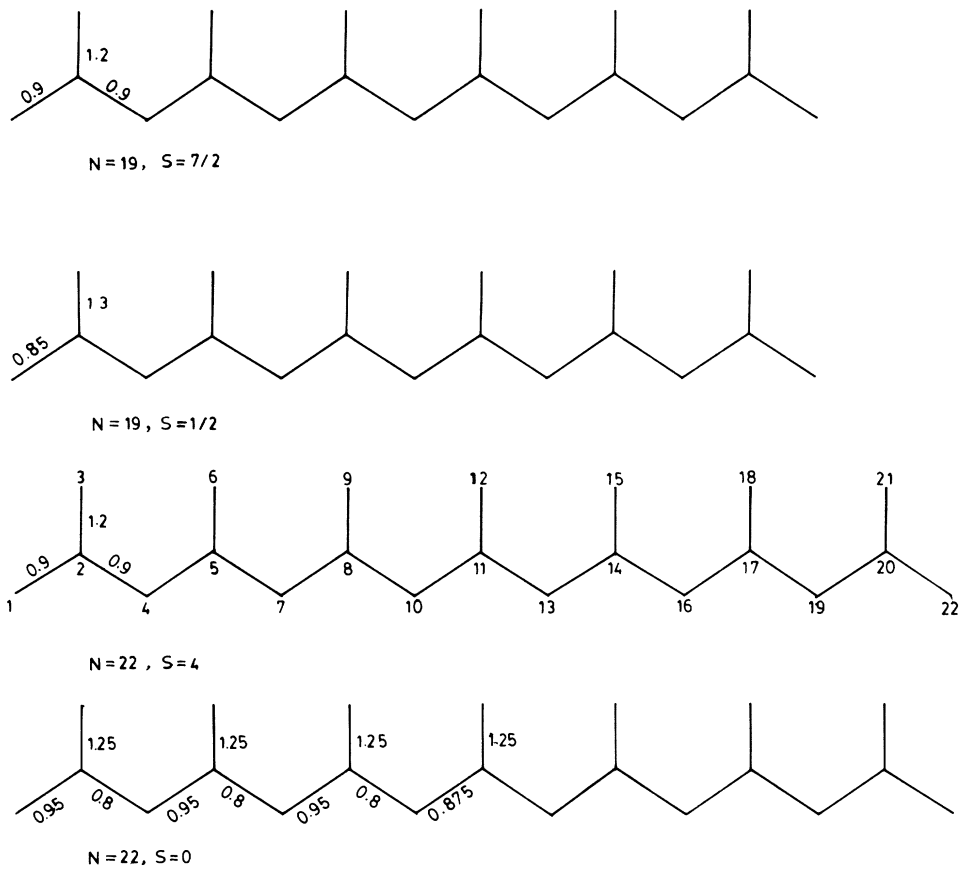

FIG. 8. Exchange integrals J of various bonds in the distorted Heisenberg model for states with spin $S=\frac{7}{2}$ and $S=\frac{1}{2}$ for the 19-spin case and $S=4$ and $S=0$ for the 22-spin case. End-to-end interchange symmetry is always assumed and where the J value is specified for fewer bonds, either uniform exchange or dimerization, as appropriate, is implied. The distortion in $N=10$ and 16 is the same as in the chain with $N=22$ while for $N=13$ the distortion is as in the $N=19$ chain.

electron. We can, therefore, describe the spin states as originating from the coupling of the effective spin of the unit cells. The state with spin S_g does not have any frustration and the bonds in the chain will be identical while the bond between the nodal atom and the dangling atom would be strongest. If we form a low-spin state with spin $S=0$, we find that if the dangling bond, which is the strongest bond, is not to be frustrated, the bonds along the chain are alternately frustrated. This is why the chain is unstable to dimerization in the low-spin state.

In Table VI we present the magnetic gap of the distorted chains along with the gap in the undistorted chains for

TABLE VIII. Spin density in different spin states in the spin model of 19 and 22 sites (Fig. 8 gives site numbering).

	$N=19$				$N=22$		
Site	$S=\frac{1}{2}$	$S=\frac{5}{2}$	$S=\frac{7}{2}$	$S=\frac{9}{2}$	$S=3$	$S=4$	$S=5$
1	−0.0894	0.4017	0.8050	0.8269	0.4396	0.8050	0.8195
2	0.0337	−0.2826	−0.5018	−0.4298	−0.2974	−0.5018	−0.4570
3	−0.0890	0.4020	0.8050	0.8270	0.4401	0.8050	0.8194
4	−0.0046	0.5058	0.7606	0.7341	0.5061	0.7606	0.7453
5	−0.0707	−0.3990	−0.5151	−0.1878	−0.3883	−0.5151	−0.2965
6	0.0686	0.5828	0.7702	0.8503	0.5675	0.7702	0.8268
7	0.2148	0.6687	0.7500	0.6286	0.6359	0.7500	0.6665
8	−0.2694	−0.4845	−0.5139	0.0631	−0.4690	−0.5138	−0.0755
9	0.4175	0.7278	0.7658	0.8964	0.6996	0.7657	0.8694
10	0.5748	0.7429	0.7486	0.5787	0.7317	0.7484	0.6067
11	−0.2695	−0.4837	−0.5139	0.0645	−0.5015	−0.5135	0.0315
12	0.4174	0.7259	0.7658	0.8966	0.7534	0.7653	0.8910

TABLE IX. Magnetic gap in the undistorted and distorted polymers in the Heisenberg model.

System size	Magnetic gap Undistorted	Distorted
7	0.1812	0.1013
10	0.2392	0.1360
13	0.1526	0.0135
16	0.1724	0.0577
19	0.1254	−0.0562
22	0.1365	0.0014

comparison. The distortion is such as to conserve the average transfer integral in the Hubbard models at 1.0 eV and in the PPP models at 2.4 eV to enable proper comparisons. Within this constraint, the transfer integrals are reassigned to each bond so as to be roughly proportional to the bond order. In Figs. 6 and 7 we give the distortion pattern used for the different spin states in the Hubbard and the PPP models. In the PPP model, the potential energy depends upon the intersite separation. The intersite separations are also adjusted by inverting the equation[22]

$$r_{p,p+1}=(-t_p+2.40\ \text{eV})/(3.21\ \text{eV})+1.397\ \text{Å}\ ,$$

which relates the transfer integral to intersite separation around the mean distance of 1.397 Å at which the transfer integral is assumed to be 2.4 eV. We find that in the distorted PPP and Hubbard chains, except for the Hubbard chain with $\varepsilon=3.0$ eV, the ground state is the low-spin state. In the Hubbard model with $\varepsilon=3.0$ eV, the site energy is comparable to the correlation energy and the bond alternation is also rather large; these conditions are unlikely to be realized in polymeric systems of the type we have considered.

We see the same behavior in the spin models as well. In Table VII we present bond orders in the central unit cell in various states for different system sizes. The bond orders in the state S_g for all system sizes correspond to a strong bond between the nodal site and the dangling site. The bond orders of the two bonds in the chain are equal. In the states with spin $S=0$ and $\frac{1}{2}$, while the strongest bond is still the bond between the nodal site and the dangling site, the $S=0$ state shows a larger alternation in the bond orders while the $S=\frac{1}{2}$ state shows a much weaker alternation. The bond orders in the state with spin S_g-1 are similar to those in the state with spin S_g. However, in the state with spin S_g+1, the bond between the nodal site and the dangling site is the weakest.

Our spin-density calculations show (Table VIII) that the total spin of the unit cell rapidly approaches one in the S_g state, and also that the ratio of the total positive-negative spin density in the unit cell indicates that there are larger positive spin densities on the dangling and the doubly bonded atoms and a more sizable negative spin density on the nodal atoms than in the Hubbard and PPP models. In the $S=\frac{1}{2}$ state the spin-density pattern in the chain corresponds to that of a soliton with most of the

TABLE X. The ratio of the bond orders (P_{ij}) to the exchange integrals (J_{ij}) for systems with $N=13$, 16, 19, in the ground and excited states in undistorted and distorted chains. The indices i and j correspond to the spin indices in Fig. 8.

N	S	Bond (i-j)	$\left[\frac{P_{ij}}{J_{ij}}\right]_{\text{uniform}}$	$\left[\frac{P_{ij}}{J_{ij}}\right]_{\text{distorted}}$
13	$\frac{1}{2}$	8-9	0.760	0.655
		7-8	0.567	0.623
		8-10	0.563	0.589
	$\frac{5}{2}$	8-9	0.725	0.662
		7-8	0.612	0.634
		8-10	0.615	0.637
16	0	8-9	0.807	0.684
		5-7	0.611	0.646
		7-8	0.524	0.676
	3	8-9	0.729	0.663
		5-7	0.609	0.634
		7-8	0.610	0.634
19	$\frac{1}{2}$	11-12	0.752	0.663
		10-11	0.583	0.613
		11-13	0.602	0.636
	$\frac{7}{2}$	11-12	0.787	0.663
		10-11	0.610	0.633
		11-13	0.610	0.634

spin density centered in the central unit cell. In the $S=S_g+1$ state, the excess spin density (relative to the $S=S_g$ state) is concentrated around the central unit cell and in the state with spin $S=S_g-1$, the spin density around the edges of the chain is reduced relative to the $S=S_g$ state, while in the middle of the chain the spin density corresponds to that in the ground state.

The chain is distorted so as to follow the bond-order patterns in the respective states, as shown in Fig. 8. The total exchange is retained so as to enable comparisons of energies. The magnetic gap in the distorted chains is presented in Table IX. We find that although the high-spin state is the ground state in the distorted chains of shorter chain length, in longer chains the ground state switches over to the low-spin state just as in the PPP and Hubbard ($|\varepsilon|=0$) models. We have recalculated the bond orders in the distorted chains to see whether the distortions introduced in the chain are close to equilibrium. Table X gives the ratio of the bond order to the exchange constant for the bonds in the distorted and the undistorted systems for spin models with $N=13$, 16, and 19 in the lowest-spin state and in the state with spin S_g. We find that this ratio is close to a constant value in the distorted chains for all the bonds for a given N and S. This implies that the distortions we have introduced in the spin models are quite close to equilibrium. Our calculation of this ratio in the PPP models showed a larger spread in the ratio although this spread was considerably smaller than in the undistorted systems.

While we have not considered the increase in lattice energy accompanying the distortion of the polymers, both in the spin models and the PPP or Hubbard models, our calculations do show that at least in the case of "soft" lattices, the high-spin state ceases to be the ground state. However, given that in one-dimension, Peierls and spin-Peierls distortions[23,24] occur independently of the stiffness of the lattice, we can say that the polymers are indeed unstable to backbone dimerization for arbitrary lattice stiffness. Thus in really long polymers of this type it is unlikely that the high-spin state will be the ground state.

IV. SUMMARY

The calculation of the energies of the different spin states of the polymers in Fig. 1 calculated employing PPP and Hubbard models shows that the high-spin state is the ground state in long-chain polymers. While the state with spin S_g-1 is nearly degenerate with the state with spin S_g, the $S=0$ or $\frac{1}{2}$ state is separated by a finite gap even in the infinite limit as shown by the calculations on the Heisenberg spin systems. The studies on the Hubbard model show that the magnetic gap is maximum for $U=4t$. Breaking the alternancy symmetry by introducing unequal site energies in the polymer only marginally reduces the stability of the high-spin ground state in the PPP model. In the Hubbard model with $U=4t$, the high-spin state ceases to be the ground state for $|\varepsilon|>2.5t$.

The bond-order calculations show that the low-spin state is susceptible to dimerization of the chain and that the bond between the nodal and the dangling site is the strongest. The spin-density pattern also suggests that the chain in the low-spin state is unstable to dimerization. The magnetic gaps in the dimerized chains show that the ground state ceases to be the high-spin state. Therefore, to succeed in the synthesis of long-chain high-spin polymers it is essential that substituents be introduced along the chain that prevent chain dimerization.

[1]J. S. Miller, A. J. Epstein, and W. M. Reiff, Chem. Rev. **88**, 201 (1988), and references therein.
[2]H. M. McConnell, J. Chem. Phys. **39**, 1910 (1963).
[3]A. Izuoka, S. Murata, T. Sugawara, and H. Iwamura, J. Am. Chem. Soc. **107**, 1786 (1985).
[4]H. M. McConnell, Proc. Robert A. Welch Found. Conf. Chem. Res. **11**, 144 (1967).
[5]T. J. LePage and R. Breslow, J. Am. Chem. Soc. **109**, 6412 (1987).
[6]T. P. Radhakrishnan, Z. G. Soos, H. Endres, and L. J. Azevedo, J. Chem. Phys. **85**, 1126 (1986).
[7]K. A. Williams, M. J. Novak, E. Dorman, and F. Wudl, Synth. Met. **19**, 709 (1987).
[8]J. B. Torrance, S. Oostra, and A. Nazzal, Synth. Met. **19**, 709 (1987).
[9]N. Mataga, Theor. Chim. Acta **10**, 372 (1968).
[10]A. A. Ovchinnikov, Theor. Chim. Acta **47**, 297 (1978).
[11]T. Sugawara, S. Bandow, K. Kimura, H. Iwamura, and K. Itoh, J. Am. Chem. Soc. **108**, 368 (1986).
[12]R. Pariser and R. G. Parr, J. Chem. Phys. **21**, 767 (1953).
[13]J. A. Pople, Trans. Farad. Soc. **42**, 1375 (1953).
[14]J. Hubbard, Proc. R. Soc. London Ser. A **276**, 238 (1963).
[15]J. H. Van Vleck, in *Quantum Theory of Atoms, Molecules and the Solid States,* edited by P.-O. Löwdin (Academic, New York, 1966), p. 475.
[16]K. Ohno, Theor. Chim. Acta (Berlin) **2**, 219 (1964).
[17]G. Rumer, Gottingen Nachrich. Tech. **1932**, 377.
[18]E. R. Davidson, J. Comput. Phys. **17**, 87 (1975).
[19]S. Rettrup, J. Comput. Phys. **45**, 100 (1982).
[20]Z. G. Soos and S. Ramasesha, in *Valence Bond Theory and Chemical Structure,* edited by D. J. Klein and N. Trinajstic (Elsevier, New York, 1990), p. 81.
[21]S. Ramasesha and P. K. Das, Chem. Phys. **145**, 343 (1990); S. Ramasesha and I. D. L. Albert, J. Phys. Chem. (to be published).
[22]L. R. Ducasse, T. E. Miller, and Z. G. Soos, J. Chem. Phys. **76**, 4094 (1982).
[23]R. E. Peierls, *Quantum Theory of Solids* (Clarendon, Oxford, 1955), p. 109.
[24]J. W. Bray, L. V. Interrante, I. S. Jacobs, and J. C. Bonner, in *Extended Linear Chain Compounds,* edited by J. S. Miller (Plenum, New York, 1983), Vol. 3, p. 353.